Geologic and geomorphic influences on the spatial extent of lateral spreading in Christchurch, New Zealand

Sarah Bastin
QuakeCoRE, University of Canterbury, Christchurch, New Zealand
Misko Cubrinovski
Civil and Natural Resources Engineering – University of Canterbury, Christchurch, New Zealand
Sjoerd van Ballegooy, James Russell
Tonkin + Taylor, Newmarket, Auckland, New Zealand

ABSTRACT
Widespread and severe lateral spreading occurred proximal to waterways during the 2010 to 2011 Canterbury Earthquake Sequence (CES). Published models for predicting lateral spread displacements have been shown to produce displacement estimates that varied by a factor of less than 0.5, to greater than 2, from those measured in parts of Christchurch following the CES. Comprehensive post-CES studies have clearly indicated that the spatial extent of lateral spreading and associated distribution of horizontal displacements along the Avon River, in eastern Christchurch, were strongly influenced by geologic and topographic features. The effect of these features is not explicitly accounted for in the current predictive models and likely contributes to some of the significant variation between predicted and measured displacements. In this study, the extent of lateral spread displacements greater than 0.5 m is derived for a study area along the Avon River from LiDAR survey and satellite imagery derived horizontal displacements. The result is cross-checked with mapped ground surface cracking, ground surveying derived horizontal displacements, liquefaction related vertical ground surface subsidence derived from LiDAR surveys, and field inspections of recorded land damage. Combining observations from each dataset enables the extent of lateral spreading to be derived while considering the measurement errors and associated limitations of each dataset. In this study, zones of lateral spreading ranging from 0 to 300 m inland from the Avon River are identified and are shown to be strongly influenced by local geomorphic features. Detailed geotechnical characterization of the subsurface soil profiles indicates that the thickness and lateral extent of the critical layers predicted to liquefy using simplified liquefaction triggering analyses directly influences the extent of lateral spreading.

1 INTRODUCTION

Liquefaction-induced lateral spreading during earthquakes poses a significant hazard to the built environment, as observed in Christchurch during the 2010-2011 Canterbury Earthquake Sequence (CES). It is critical that geotechnical engineers are able to adequately assess lateral spreading extents and associated displacements for design purposes. Published empirical and semi-empirical models for predicting lateral spread displacements have been shown to produce displacement estimates that varied by orders of magnitude from those recorded in parts of Christchurch following the CES (i.e. Bowen et al. 2012, Deterling, 2015, Cubrinovski and Robinson, 2016, Russell et al. 2017). These predictive models were typically derived from limited case histories and relatively small geotechnical datasets as the researchers undertaking this work were frequently limited in the resources available (e.g. Youd et al. 2002, Zhang et al. 2004). In addition, it has often been difficult to estimate the extent and magnitude of horizontal ground displacements post-event, thus adding additional uncertainties to the development of these prediction methodologies.

Widespread and severe lateral spreading occurred proximal to waterways during the September 2010 M_w 7.1 Darfield and subsequent February 22nd 2011 M_w 6.2 Christchurch earthquakes (Fig. 1A) (GEER, 2010, 2011). Minor lateral spreading was also reported following the June 2011 M_w 5.9 and December 2011 M_w 5.9 earthquakes. Extensive LiDAR survey derived horizontal ground displacements are available for each of the main CES earthquakes and across the CES (Tonkin and Taylor, 2015). Satellite imagery derived displacements are also available for the February 2011 earthquake and the CES (Martin and Rathje, 2014). These datasets provide an indication of the maximum likely extent of lateral spreading, and the associated magnitude and direction of ground movement. However, each dataset has inherent limitations including spatial resolution, accuracy, and acquisition errors (i.e. flight line offset). Additional datasets including liquefaction related vertical ground surface subsidence derived from LiDAR surveys, ground surveying of lateral spread displacements, and documented land damage provide additional information on the extent of lateral spreading. Combining observations from multiple datasets provides a unique opportunity to resolve the maximum extent of lateral spreading for the CES. The use of multiple independent forms of measurement allow for the limitations and/or acquisition errors of each dataset to be manually filtered. The extensive and detailed observations that can be made from multiple data sources across the CES provides a high quality case history database that spans multiple events (i.e. GEER, 2010 and 2011; Martin and Rathje, 2014; Bastin et al. 2015; and Cubrinovski and Robinson, 2016). Extensive post-CES geotechnical data provides an additional opportunity to characterize the subsurface soil profiles in areas with significant lateral spreading, and areas of negligible to no lateral spreading.

In this study, the extent of lateral spreading induced horizontal displacements greater than 0.5 m is derived for

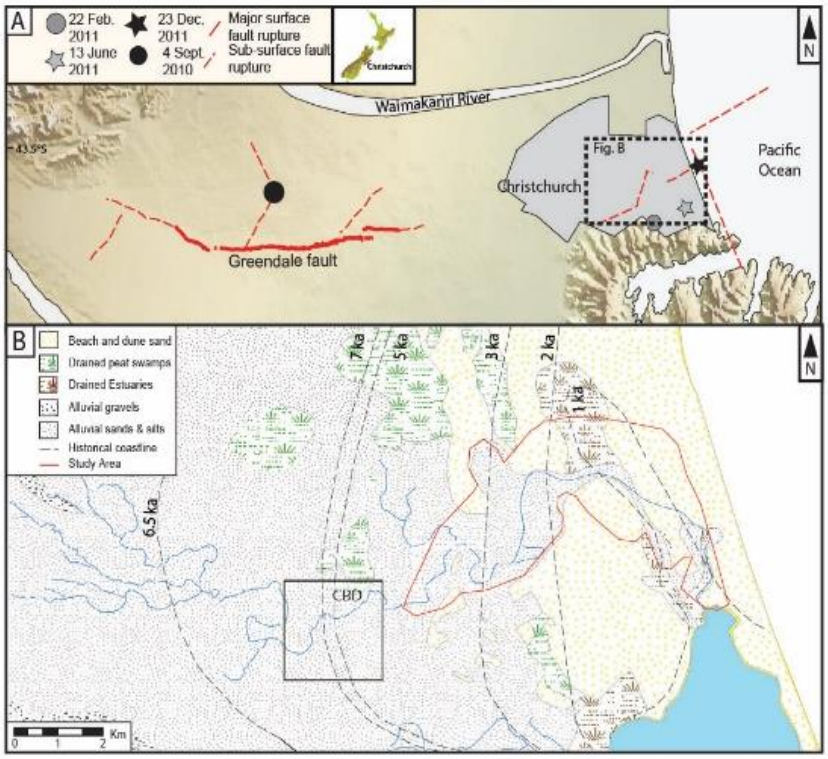

Fig. 1: A) Epicentral locations of the liquefaction triggering earthquakes of the 2010-2011 Canterbury Earthquake Sequence with fault ruptures indicated (Modified from Bastin et al. 2015). B) Simplified geological map of the Christchurch area with the approximate location of historical coastlines with respect to the Central Business District (CBD) and study area indicated (modified from Brown and Weeber, 1992)

a study area in eastern Christchurch using the extensive post-event datasets. The result is compared with local geologic and geomorphic variability while detailed geotechnical characterization is undertaken in selected areas.

2 GEOLOGIC AND GEOMORPHIC SETTING

The city of Christchurch (population 360,000) is primarily situated upon a low relief alluvial landscape on the east coast of New Zealand's South Island. The central and eastern suburbs of the city are predominantly underlain by alluvial sands, silts, and drained peat swamps which are locally interbedded with dune, estuarine, and fore-shore sands to silts (Fig. 1B) (Brown and Weeber, 1992). The alluvial sands and silts were initially deposited by the Waimakariri River, which regularly flooded and avulsed across the region prior to European settlement (Fig. 1B). Sediments were subsequently reworked and re-deposited by meandering rivers (i.e. Avon River) that also flooded and avulsed across the area now occupied by Christchurch (Fig. 1) (Brown and Weeber, 1992). The dune, estuarine, and foreshore sands to silts were deposited during sea level regression following a mid-Holocene high-stand that reached up to 3 km inland of the central city at 6,500 years before present (Fig. 1B) (Brown and Weeber, 1992). The youthful unconsolidated nature of these predominately-fine sands and silts combined with a shallow groundwater water table (typically 1-2 m depth) pose a long recognized, high liquefaction hazard for much of the city (Elder et al. 1991). West of the central city is predominantly underlain by fluvial sands and gravels (Fig. 1B) (Brown and Weeber, 1992).

The study area is located along the Avon River in eastern Christchurch, as indicated in Fig. 1B. The area is underlain by alluvial sands and silts, along with drained estuarine and swamp deposits. The landscape within the study area is dominated by landforms associated with the development of the meandering Avon River and interaction with paleo-coastlines (Fig. 1B).

3 METHODOLOGY

3.1 Deriving the extent of lateral spreading displacements

Lines encompassing the inland extent of horizontal displacements greater than 0.5 m were manually derived from the CES LiDAR survey and satellite datasets (Fig. 2). Care was taken to ensure that only areas that spread towards the river were included within the extent. Areas where the direction or extent of lateral spreading appeared to be complicated by local topographic and/or geomorphic features such as paleo-channels, active streams, and sloping of ground away from the river were excluded from this initial assessment. The derived lines from each dataset were subsequently superimposed and a smoothed line depicting the extent lateral spread displacements greater than 0.5 m was derived (Fig. 2).

LiDAR survey derived horizontal displacements were calculated from comparison of the horizontal position of objects (i.e. buildings) in LiDAR survey point clouds created from pre- and post- event surveys. Displacements were calculated using a sub-pixel correlation method developed by Imagin'Labs Corporation and California Institute of Technology (Tonkin and Taylor, 2015). The liquefaction related component of the horizontal displacements was derived by subtracting the horizontal

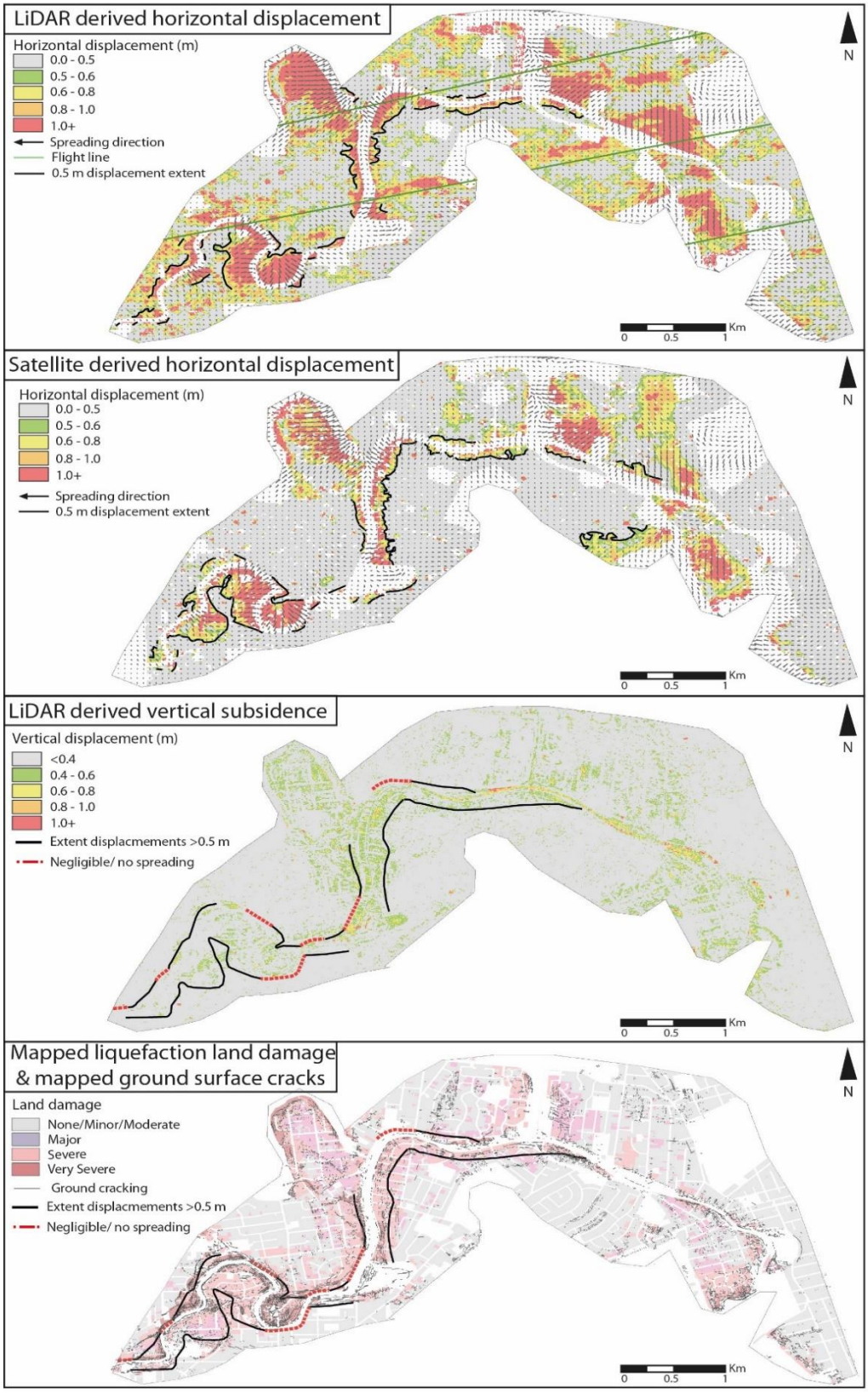

Fig. 2: Lines marking the inland extent of displacements greater than 0.5 m were derived from the LiDAR survey and satellite derived horizontal displacements. A smoothed line depicting the maximum inland extent of lateral spread displacements greater than 0.5 m was derived from comparison of these two lines. The resultant line was cross-checked against mapped ground surface cracking, LiDAR survey derived liquefaction related vertical ground surface subsidence, and recorded land damage.

regional tectonic deformation from the fault rupture model by Beavan et al. (2012). Metadata supplied with the source LiDAR survey indicates that the horizontal accuracy is in the order of 0.40 to 0.55 m. Displacements less than 0.5 m are considered to be within the error range and are therefore excluded from analysis. Localized offsets along the LiDAR survey flight lines are recognizable as error bands resulting in anomalous displacement magnitudes and directions; displacements proximal to these bands were not considered in the analysis.

Satellite imagery derived horizontal displacements were measured from pre- and post- event satellite imagery using an optical imagery correlation process conducted by Martin and Rathje (2014). Analyses were performed using a chip window of 128 by 128 pixels and a step size of 32 pixels, which produced a displacement estimate every 16 m. Results with a signal to noise ratio less than 0.95 were removed and displacements less than the root mean square error of 0.30 m were set as zero. The satellite-derived displacements are based on local displacements relative to areas distal to the rivers that did not laterally spread. The horizontal tectonic displacements are therefore not included in these derived displacements and hence no adjustments are required. The accuracy of the satellite imagery derived displacements is 0.3 m however, displacements greater than 0.5 m are primarily considered to ensure consistency with the LiDAR survey.

The line depicting the inland extent of lateral spread displacements greater than 0.5 m was cross-checked against liquefaction related vertical ground surface subsidence as derived from LiDAR surveys, recorded land damage, ground surveyed lateral spread displacements, and mapped ground surface cracking (Fig. 2). The liquefaction related ground surface subsidence was calculated from comparison of pre- and post- event Digital Elevation Models (DEM) developed from the LiDAR surveys with the regional vertical tectonic deformation from Beavan et al. (2012) subtracted (Tonkin and Taylor, 2013). The liquefaction related ground surface subsidence provides a crude indication of the extent of lateral spreading as subsidence is also caused by liquefaction related volumetric consolidation and loss of soil volume due to ejecta, in addition to the lateral spreading induced ground surface settlement. As a result, the dataset was used for cross-checking purposes only. The extent of lateral spread displacements greater than 0.5 m was additionally cross-checked with land damage documented for each residential property by Tonkin + Taylor Ltd during post-event reconnaissance and surveying for the EQC (Tonkin and Taylor, 2013). Land classified as experiencing major to very severe damage and that spread towards the river was generally included within the extent (Fig. 2). The damage categories refer to the amount of ejected material, the severity of ground cracking, and evidence of lateral displacement at the site (refer to Tonkin and Taylor, 2013 for discussion on the field mapping and classification).

Lateral spreading induced horizontal displacements measured from ground survey transects by Cubrinovski and Robinson (2016) were additionally used to cross-check the derived line. Ground surface cracking mapped by Tonkin and Taylor Ltd. during post-event reconnaissance and available from the New Zealand Geotechnical Database (NZGS, 2017) were additionally used for cross-checking.

3.2 Geomorphic mapping

The geomorphology of the study area was mapped from subtle variations in topography and in the shape and morphology of the Avon River, as observed within the 0.5 m DEM of the area (Fig. 3B). The result was supplemented and cross-checked with the simplified geological map of Christchurch (Brown and Weeber, 1992) and initial drainage maps of the city (Christchurch City Council, 1856). The 0.5 m DEM was downloaded from the New Zealand Geotechnical Database (NZGD, 2017).

3.3 Geotechnical characterization of geomorphic and lateral spreading zones

Cone Penetration Tests (CPT) available from the NZGD were assessed for selected transects within the study area for detailed geotechnical characterization of the subsurface soil profiles. Transects were selected in areas of negligible to no lateral spreading, and in areas where lateral spreading did occur and was not complicated by river geometry (i.e. meander bends). The selected transect locations are shown in Fig. 4.

The likelihood of liquefaction for the ground accelerations and depth to the ground water table of the February 2011 earthquake were calculated for each CPT using the Boulanger and Idriss (2014) methodology. The sediment behaviour-type index (I_c) threshold of greater than 2.6 was applied, above which the soil was assumed too plastic in behaviour to liquefy (Robertson and Wride, 1998). The Fines Content (FC) was estimated from the I_c using the Boulanger and Idriss (2014) correlation with a fitting parameter C_{FC} value of 0.1 selected based on the studies by Lees et al. (2015). Further analysis will incorporate the FC correlation derived for the Avon River by Cubrinovski and Robinson (2016).

4 GEOMORPHOLOGY OF THE STUDY AREA

The Avon River and surrounding alluvial plain is typical of a meandering river (Fig. 3B). The sinuosity of the river forms meander-bends, the outer-banks of which contain remnant high ground that is eroded during bank-full condition as the highest flow velocities are concentrated towards these banks. Eroded sediments are subsequently transported and deposited on the inner bank as point-bar deposits comprising fine sand grading to silt. The inner-meander bends exhibit low-elevations proximal to the river that generally increase with distance from the channel as a result of point-bar deposit accumulation and the associated outward migration of the meander-bend. Cut-off meander bends and associated paleo-channels are also present within the study area and represent former meander bends cut-off from the main channel during rapid channel avulsion (Fig. 3B). The cut-off meander-bend and associated paleo-channel labelled as Horseshoe Lake in Fig. 3B is recognized as a depression in the landscape which complicates the topographic profile along the river. The

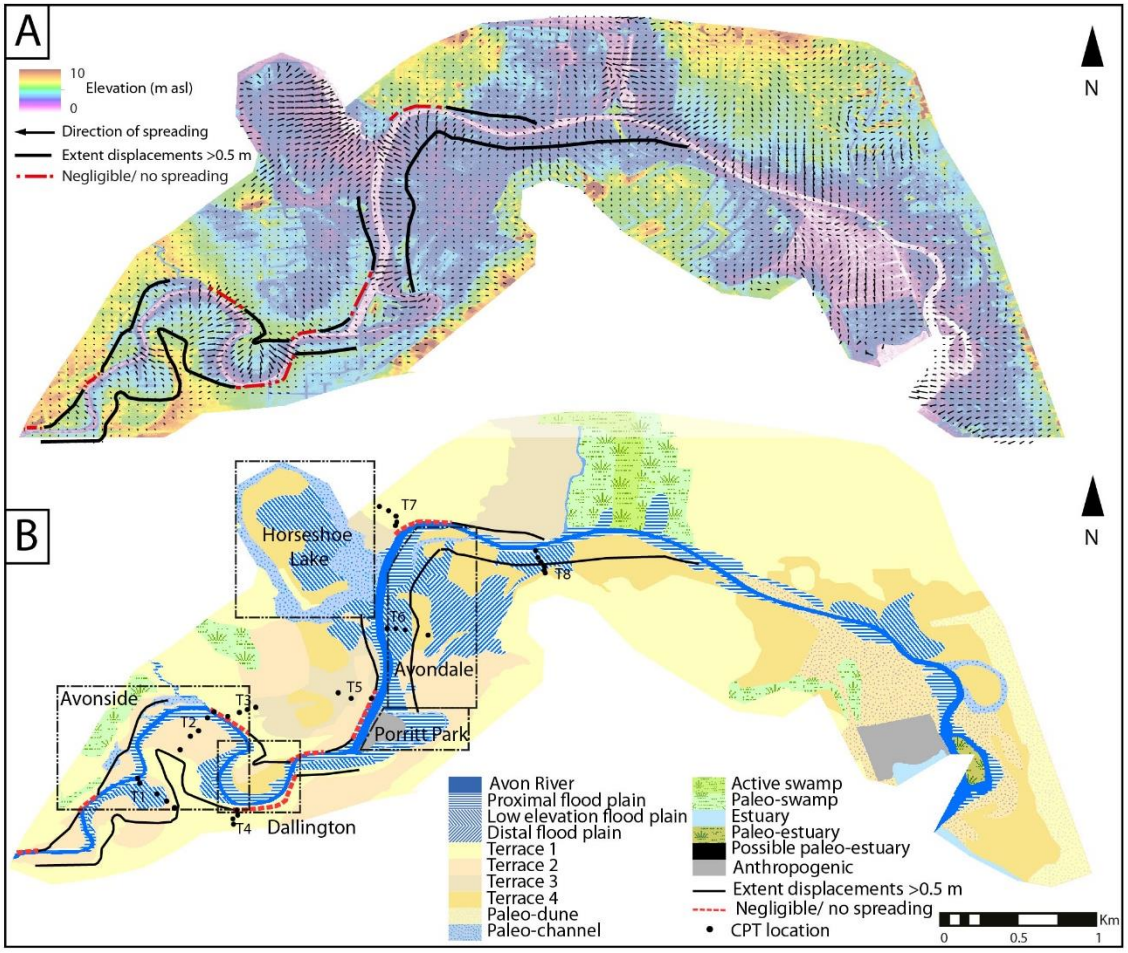

Fig. 3: A) 0.5 m DEM of the study area overlain with the line depicting the maximum extent of lateral spread displacements greater than 0.5 m, and vectors indicating the direction of spreading. B) Comparison of the line depicting the extent of displacements greater than 0.5 m with local geomorphic variability. Lateral spreading is observed within areas re-worked by the river, while negligible to no lateral spreading is observed in the remnant, higher elevation ground. The locations of transects 1-8 plotted in Fig. 4 are also indicated.

meander bend adjacent to Porritt Park (indicated in Fig. 3B) was anthropogenically cut-off from the main channel to straighten the river for improved rowing training.

The alluvial plain surrounding the river is underlain by fine sand to silt deposited as the river over-topped its bank during flood events (Fig. 3). Localized areas of low elevation within the flood plain may be associated with paleo-channels of the river and/or tributary streams. Early maps of Christchurch indicate that these depressions contained swamps, which most likely formed as water pooled in these areas following flood events (Christchurch City Council, 1856).The alluvial landscape is locally truncated by remnant higher ground that has not been eroded or re-worked by the river (Terrace 1; Fig. 3B) (Brown and Weeber, 1992).

Remnants of the ~1,000 year before present estuary is observed at the eastern extent of the study area and corresponds with areas of very low elevation (Fig. 3). Initial maps of the city indicate that swamps formed in these areas, most likely as a result of water pooling following flood events (Brown and Weeber, 1992).

The interaction of the fluvial and marine depositional processes within the eastern reaches of the study area complicates the surface morphology and results in significant spatial heterogeneity in the subsurface soils.

5. COMPARISON OF THE EXTENT OF LATERAL SPREADING BETWEEN GEOMORPHIC AREAS

The extent of lateral spreading within the eastern section of the study area appears to be complicated by local geomorphic variability, as a result, the extent of lateral spreading was not analyzed in this area (Figs. 2 and 3). Lateral spreading adjacent to the low-elevation paleo-estuary appears to be influenced by the sloping of the ground away from the river, with horizontal displacements directed away from the river (Figs. 2 and 3).

The geomorphology of the western extent of the study area is dominated by active and cut-off meander bends of the Avon River (Fig. 3B). The extent of lateral spread displacements greater than 0.5 m was able to be derived for the active meander bends. The distribution and orientation of lateral spreading proximal to the cut-off

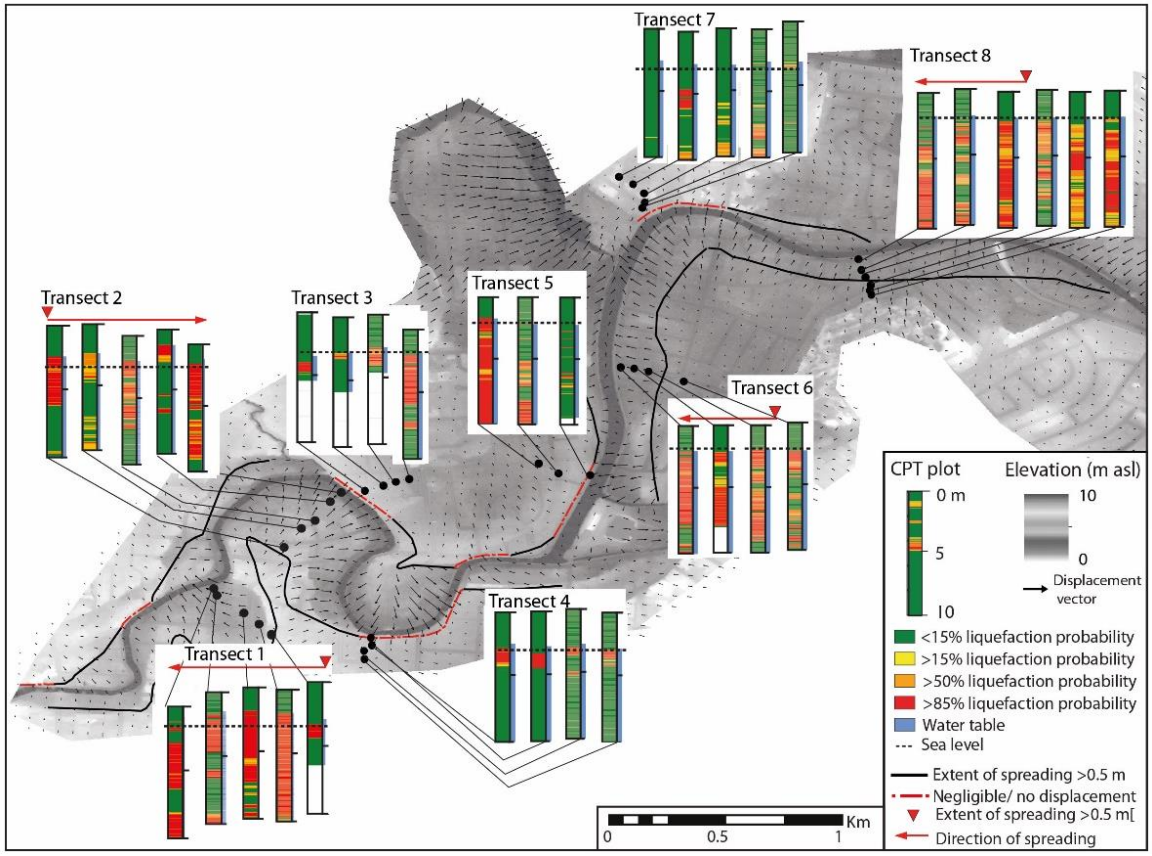

Fig. 4: Transects with plots outlining the soil layers predicted to liquefy for the February 2011 earthquake as derived from simplified analysis of the CPT (positions indicated). Plots are shown with respect to sea level (dashed line) and the extent of lateral spread displacements greater than 0.5 m. Areas that laterally spread are shown to be underlain by comparably thick profiles of liquefying soil. Areas of negligible to no spreading generally contain thin to non-existent liquefying soil layers overlain by thick non-liquefying soil layers.

meander bends is complicated by the paleo-channels which result in localized depressions distal to the river (Figs. 2 and 3). The extent of lateral spreading is therefore not analyzed adjacent to the cut-off meander bends (Fig. 3).

The inland extent of lateral spread displacements greater than 0.5 m is shown to vary between the inner and outer-banks of the active meander bends within the study area (Fig. 3). Areas with displacements less than 0.5 m correspond with remnant high ground (Terrace 1) on the outer-banks of the river and are downstream from the apex of the meander bend (Fig. 3). The change in river orientation at the apex of the meander bend directs water flow towards the outer bank thus promoting erosion; sediment deposition generally does not occur in these areas.

Localized lateral spreading extending approximately 200 m inland is observed within the low-to-mid elevation flood plain on the outer-banks of the river upstream from the apex of the meander bends (Fig. 3). The river morphology indicates that these areas would be re-worked and receive sediment as water is forced around the apex of the meander bend during flood events. The subsurface soil profiles therefore likely contain unconsolidated fluvial sediment that is potentially liquefiable.

The extent of lateral spread displacements greater than 0.5 m within the inner-meander bends generally extends 300 to 400 m inland, however appears to be complicated by changes in river orientation and local topographic variability (Fig. 3). Lateral spread displacements greater than 0.5 m within Avonside generally appear to be confined to the lower elevation flood plains and terraces (indicated in Fig. 3). The ridge of remnant higher elevation ground (Terrace 1) that locally transects the bend complicates the pattern of lateral spreading in this area (indicated in Fig. 3). Lateral spread displacements greater than 0.5 m within the inner-meander bend comprising Dallington appears to be constrained by the transition into the remnant higher elevation ground (Terrace 1 indicated in Fig. 3). The deposition of point-bar deposits along the inner meander bend and associated out-ward migration of the bend results in thick successions of loose, unconsolidated sediments that are potentially liquefiable and therefore likely facilitated lateral spreading.

The zone of lateral spread displacements greater than 0.5 m within Avondale extends approximately 350 m inland and appears to be locally influenced by the terraces intersecting the area (marked in Fig. 3). The overall low elevations of the area indicate that the area is located within the flood plain of the river and is therefore likely

underlain by unconsolidated fine sand inter-layered with silts deposited between flood events.

The comparison of the inland extent of lateral spread displacements greater than 0.5 m and local geomorphic variability indicates that there is a strong link between depositional setting and the extent of lateral spreading. Local geomorphic variability is shown to explain factors resulting in anomalous lateral spreading patterns (i.e. paleo-estuaries and cut-off meander bends).

6. GEOTECHNICAL CHARACTERISTICS OF GEOMORPHIC AREAS AND LATERAL SPREADING AREAS

The predicted liquefaction of the soil profiles for the February 2011 earthquake is evaluated for comparison with the inland extent of lateral spread displacements greater than 0.5 m. Eight CPT transects were selected and analyzed within the study area (shown in Fig. 4). The depth and thickness of the liquefying layers is visually compared with the extent of lateral spread displacements greater than 0.5 m. The location of each transect with respect to the geomorphic areas is indicated in Fig. 3; Transects 1, 2, 6, and 8 are located in areas where lateral spread displacements greater than 0.5 m occurred, whereas transects 3, 4, 5, and 7 are in areas where negligible to no lateral spreading was observed.

Transect 1 is located within the Avonside inner meander bend; the transect crosses from the low elevation flood-plain into the mid-elevation Terrace 2, and the remnant high ground comprising Terrace 1 (Fig. 3). The zone of displacements greater than 0.5 m appears to cease just back from the riser between Terraces 1 and 2 (Fig. 4). The CPT within the low elevation flood plain and Terrace 2 indicate that the area is underlain by a thick profile of soil that was liquefiable during the February earthquake (Fig. 4). In comparison, the CPT on Terrace 1, is shown to contain comparably much thinner liquefying soil layers (Fig. 4). The change in elevation, soil characteristics, and liquefiable layer thickness across the terrace riser likely influenced the inland extent of lateral spread displacements greater than 0.5 m (Fig. 4).

Transect 2 extends across the active flood plain of the river, and across Terrace 2 (Fig. 3). The zone of displacements greater than 0.5 m appears to cease approximately along the riser into Terrace 1 (Fig. 3). The CPT indicate that the area is generally underlain by a thick layer of liquefying soils. The exception to this is the second CPT, which contains only a thin layer of liquefying soil (Fig. 3). It is likely that the extent of lateral spread displacements greater than 0.5 m in this area was controlled by the relative change in the thickness of the liquefying soils over a large area.

Transect 3 is located within remnant higher elevation ground (Terrace 1) in an area of negligible to no lateral spreading during the CES (Fig. 3). The CPT proximal to the river indicate that the subsurface sediment contains thin layers at ~3-3.5 m depth that are predicted to liquefy during the February 2011 earthquake by the simplified triggering analysis. The CPT distal to the river contains a thicker liquefying layer, albeit is located in a lower elevation depression (Terrace 3) (Fig. 3B). Standing water likely pooled in this area following floods resulting in the deposition of the fine sediments that are liquefiable. The lack of liquefying soil layers within the area proximal to the river (Terrace 1) likely prevented extensive lateral spreading from occurring within Terrace 3 (Figs. 3 and 4).

Transect 4 is also located within Terrace 1 within an area of negligible to no lateral spreading (Fig. 3). The CPT indicate that the subsurface sediment contains a comparably thin layer of soil at 3.2-3.5 m depth that is predicted to liquefy (Fig. 4). The lack of significant lateral spreading at the site combined with presence of thin layers that are predicted to liquefy, suggests that the simplified triggering methodology may have over-predicted liquefaction within this area.

Transect 5 is located in an area of negligible to no lateral spreading within the mid-elevation Terrace 2 (Fig. 3). The river in this location was anthropogenically straightened, causing the opposite meander bend to be abandoned (see Porritt Park; Fig. 3B). The transect location was therefore not formerly located adjacent to the river, which combined with the overall higher elevations of the area, indicate that the area is not underlain by recent fluvial sediments. The CPT indicate that the soil profiles proximal to the river were not predicted to liquefy (Fig. 4). It is noted that the CPT conducted distal to the river and within the lower elevation back-swamp of Terrace 3 contains a thick layer of liquefying soil (Fig. 3 and 4). The lack of liquefying soil layers within the area proximal to the river (Terrace 1) likely prevented significant lateral spreading from occurring within Terrace 3 (Fig. 3). Conversely, minor lateral spreading appeared to occur away from the river in this area, likely as a result of decreasing elevation away from the river combined with the thickening profile of liquefying soils.

Transect 6 crosses from the very low-elevation distal flood plain of the Avon River into Terrace 4 (Fig. 3B). The area proximal to the river experienced lateral spread displacements greater than 0.5 m during the CES (Fig. 3A). The CPT within the area of displacements greater than 0.5 indicate that the subsurface sediment contains comparably thick layers of liquefying soil (Fig. 4). The CPT conducted outside of the area with displacements greater than 0.5 indicate that the thickness of liquefying soil decreases and becomes inter-layered with non-liquefying soil (Fig. 4). It is possible that this area experienced displacements less than 0.5 m. The decreasing rates of lateral spreading with increasing distance from the river likely result from the decreasing thickness of the liquefiable layer combined with the low gradient of the area (Fig. 4).

Transect 7 is located adjacent to an outer-meander bend of the river within remnant higher ground (Terrace 1) which experienced negligible to no lateral spreading (Fig. 3). The CPT indicate that the soil profile does not contain liquefying soil layers for the February earthquake. Therefore limiting lateral spreading at this location.

Transect 8 is located within the low elevation flood plain (Fig. 3). The CPT indicate that the soil profiles within, and outside of the zone of lateral spread displacements greater than 0.5 m contain relatively uniform and comparably thick layers of liquefying soils (Fig. 4). It is likely that displacements less than 0.5 occurred outside the identified zone, and that the decreasing rates of displacement with

increasing distance from the river result from the low gradient and free-face height of the area.

Comparison of the extent of lateral spreading across the study area indicates that the thickness and continuity of the liquefying soil layers directly influenced the extent of lateral spread displacements greater than 0.5 m. The thickness and extent of the liquefying soil layers can be directly attributed to depositional characteristics associated with the development of the meandering Avon River. Negligible to no lateral spreading is observed within remnant higher elevation ground that contains thin or inter-layered liquefiable layers (Transects 3, 4, 5 and 7; Fig. 4). These areas have not been re-worked by the Avon River and subsequently do not receive unconsolidated fluvial sediments during flood events. In comparison, lateral spread displacements greater than 0.5 m are observed within the active and low- to mid- elevation flood plains of the river (Terraces 2-4; Fig. 3). These areas likely received sediment during flood events and are underlain by comparably thick layers of liquefying soil (Transects 1, 2, 6 and 8; Fig. 4). The presence of thick layers of liquefying soil proximal to the river in these areas facilitated the significant lateral spreading observed in these areas.

7. CONCLUSIONS

The extent of lateral spread displacements greater than 0.5 m is derived for a study area in eastern Christchurch for the Canterbury earthquake sequence from post-event LiDAR survey and Satellite imagery derived horizontal displacements. The resultant line was cross-checked with liquefaction related vertical ground surface subsidence derived from LiDAR surveys, field inspections of land damage, ground surveyed lateral spread displacements, and mapped ground cracking. The extensive and detailed observations that can be made from multiple data sources across the CES provides a high quality case history database that spans multiple events.

The inland extent of lateral spread displacements greater than 0.5 m is shown to be strongly influenced by local geomorphic variability within the study area. Lateral spreading appears to be confined to the low to mid elevation flood-plain which receives sediment during flood-events and is subsequently underlain by unconsolidated fluvial fine sand to silt. In comparison, negligible to no lateral spreading is observed where remnant high ground is located proximal to the river bank. These areas are eroded by the river and are not underlain by recent unconsolidated fluvial sediment. It is noted that the presence of paleo-channels, cut-off meander bends, and paleo-estuaries complicates the pattern and distribution of lateral spreading and associated ground deformation within the study area.

Simplified liquefaction triggering analyses of the CPT at February 2011 levels of earthquake shaking, indicate that the depth and thicknesses of the liquefying soil influences the extent and severity of lateral spreading. Lateral spread displacements greater than 0.5 m correlate with areas underlain by thick and continuous liquefiable layers, while negligible to no displacement occurs where liquefying layers are thin and/or inter-layered with non-liquefying layers. Analysis of the CPT using the simplified liquefaction triggering analysis provides some consistency between the characteristics of the soil profiles that did and did not result in significant lateral spread displacements within the study area.

Further work is required to characterize the variability in the subsurface sediment types and liquefying layers across the study area and scrutinize the link with the likely extent and magnitude of lateral spreading. Future work plans to conduct detailed characterization of the soils proximal to the eight transects, and further examine the mechanism facilitating lateral spreading in conjunction with the study by Cubrinovski and Robinson (2016).

8. ACKNOWLEDGEMENTS

This project was supported by QuakeCoRE, a New Zealand Tertiary Education Commission-funded Centre. This is QuakeCoRE publication number 0134. The Ministry of Building, Innovation and Employment provided additional support for supplementary CPT within the study area.

9. REFERENCES

Bastin, S. H., Quigley, M. C. and Bassett, K. 2015. *Comparison of Liquefaction-induced Land Damage and Geomorphic Variability, Avonside, New Zealand.* 6th International Conference on Earthquake Geotechnical Engineering, Christchurch, New Zealand.

Beavan, J., Motagh, M., Fielding, E., Donnelly, N. and Collett, D. 2012. Fault slip models of the 2010-2011 Canterbury, New Zealand, earthquakes from geodetic data and observations of post-seismic ground deformation. *New Zealand. Journal of Geology and Geophysics*, 55(3):207-221.

Boulanger, R. and Idriss, I. 2014. *CPT and SPT based liquefaction triggering procedures, Report No. UCD/CGM-14/01.* Center for Geotechnical Modelling, Department of Civil and Environmental Engineering, University of California Davis, California.

Bowen, H., Jacka, M., van Ballegooy, S., and Sinclair, T. 2012. *Lateral spreading in the Canterbury earthquake - observations and empirical prediction methods.* Proceedings, 15th World Conferences on Earthquake Engineering (WCEE), Lisboa, Portugal.

Brown, L. and Weeber, J. 1992. *Geology of the Christchurch Urban Area. Scale 1:25 000*. Institute of Geological and Nuclear Sciences geological map 1. 1 sheet + 105 p, Lower Hutt, New Zealand.

Christchurch City Council (1856). *Black Map of Christchurch,* Archives New Zealand.

Cubrinovski, M. and Robinson, K. 2016. Lateral spreading: Evidence and interpretation from the 2010-2011 Christchurch earthquakes, *Soil Dynamics and Earthquake Engineering*, 91: 187–201.

Deterling, O. 2015. *Factors influencing the lateral spread displacements from the 2011 Christchurch, New Zealand earthquake*. M.Sc. in Engineering Thesis, University of Texas at Austin, United States of America.

Elder, D., McCahon, I. and Yetton, M. 1991. *The earthquake hazard in Christchurch: a detailed evaluation.* Research Report to the EQC: Soils and Foundations Ltd., New Zealand.

GEER 2010. *Geotechnical Reconnaissance of the 2010 Darfield (New Zealand) Earthquake. Version 1: November 14, 2010*, Report of the National Science Foundation – Sponsored Geotechnical Extreme Events Reconnaissance (GEER) Team.

GEER 2011. *Geotechnical Reconnaissance of the 2011 Christchurch, New Zealand Earthquake. Version 1: November 8, 2011,* Report of the National Science Foundation – Sponsored Geotechnical Extreme Events Reconnaissance (GEER) Team.

Lees, J., van Ballegooy, S., and Wentz, F. 2015. Liquefaction Susceptibility and Fines Content Correlations of Christchurch Soils. *6th International Conference on Earthquake Geotechnical Engineering*, Christchurch, New Zealand.

Martin, J. G. and Rathje, E. M. 2014. Lateral Spread Deformations from the 2011 Christchurch, New Zealand Earthquake Measured from Satellite Images and Optical Image Correlation. *10th National Conference in Earthquake Engineering, Earthquake Engineering Research Institute (EERI)*, Anchorage.

Robertson, P. and Wride, C. 1998. Evaluating cyclic liquefaction potential using the cone penetration test. *Canadian Geotechnical Journal,* 35(3):442- 459.

Russell, J., van Ballegooy, S., Ogden, M., Bastin, S., Cubrinovski, M. 2017. Influence of geometric, geologic, geomorphic and subsurface ground conditions on the accuracy of empirical models for prediction of lateral spreading, *Paper submitted to the 3rd International Conference on Performance-based Design in Earthquake Geotechnical Engineering*, Vancouver, BC, Canada, July 16-19.

Tonkin and Taylor 2013. *Liquefaction Vulnerability Study*. Report prepared for Earthquake Commission, New Zealand.

Tonkin and Taylor 2015. *Canterbury Earthquake Sequence: Increased Liquefaction Vulnerability Assessment Methodology***,** Report prepared for Earthquake Commission, New Zealand.

Youd, T. L., Hansen, C. M. and Bartlett, S. F. 2002. Revised multi-linear regression equations for prediction of lateral spread displacement. *Journal of Geotechnical and Geoenvironmental Engineering,* 12(128): 1007-1017.

Zhang, G., Robertson, P. K. and Brachman, R. W. I. 2004. Estimating Liquefaction-Induced Lateral Displacements Using the Standard Penetration Test of Cone Penetration Test. *Journal of Geotechnical and Geoenvironmental Engineering*, 8(130): 861-871.